Genomic glucocorticoid receptor effects guide acute stress-induced delayed anxiety and basolateral amygdala spine plasticity in rats.

Leonardo S. Novaes[1], Leticia M. Bueno-de-Camargo[1], Amadeu Shigeo-de-Almeida[1], Vitor A. L. Juliano[1], Ki Goosens[2], Carolina D. Munhoz[1*].

[1]Department of Pharmacology, Universidade de Sao Paulo Instituto de Ciencias Biomedicas, São Paulo, Brazil, 05508-000.

[2]Department of Psychiatry, Icahn School of Medicine at Mount Sinai, New York, NY 10029.

*Carolina Demarchi Munhoz

Email: cdmunhoz@usp.br

Author Contributions: LSN: designed research, performed research, analyzed data, wrote the paper; LMBC: performed research, analyzed data; ASA: performed research, analyzed data; NBS: performed research, analyzed data; KG: designed research, contributed unpublished reagents/analytic tools, wrote the paper; CDM: designed research, analyzed data, contributed unpublished reagents/analytic tools, wrote the paper.

Competing Interest Statement: The authors declared no conflicts of interest concerning their authorship or the publication of this article.

Keywords: restraint; neuroplasticity; amygdala; glucocorticoid signaling; anxiety; behavior.

Abstract

Anxiety, a state related to anticipatory fear, can be adaptive in the face of environmental threats or stressors. However, anxiety can also become persistent and manifest as anxiety- and stress-related disorders, such as generalized anxiety or post-traumatic stress disorder (PTSD). In rodents, systemic administration of glucocorticoids (GCs) or short-term restraint stress induces anxiety-like behaviors and dendritic branching within the basolateral complex of the amygdala (BLA) ten days later. Additionally, increased arousal-related memory retention mediated by elevated GCs requires concomitant noradrenaline (NE) signaling, both acting in the BLA. It is unknown whether GCs and NE play a role in the delayed acute stress-induced effects on behavior and BLA dendritic plasticity. Here, inhibiting corticosterone (CORT) elevation during two hours of restraint stress prevents stress-induced increases in delayed anxiety-like behavior and BLA dendritic spine density in rats. Also, we show that the delayed acute stress-induced effects on behavior and morphological alterations are critically dependent on genomic glucocorticoid receptor (GR) actions in the BLA. Unlike CORT, the pharmacological enhancement of NE signaling in the BLA was insufficient to drive delayed anxiety-related behavior. Nonetheless, the delayed anxiety-like behavior ten days after acute stress requires NE signaling in the BLA during stress exposure. Therefore, we define the essential roles of two stress-related hormones for the late stress consequences, acting at two separate times: CORT, via GR, immediately during stress and NE, via beta-adrenoceptors, during the expression of delayed anxiety.

Significance Statement

The dysregulation in orchestrating and finetuning major stress-related neural circuitries leads to enhanced reactivity and other altered ways of coping with threatening situations, predisposing humans to multiple psychiatric disorders, including anxiety and PTSD. Given the tremendous burden of affective disorders, we must advance our understanding of stress neurobiology and translate this into improved treatments. Here we showed that the absence of neuronal genomic GR signaling in the BLA prevented delayed effects on anxiety-like behavior and dendritic spine density ten days after stressor exposure. We also demonstrate that CORT, via GR and immediately at stress and NE, via beta-adrenoceptors, during the expression of delayed behavior contribute to the late stress consequences.

Introduction

The body's physiological and behavioral responses to stressful stimuli have critical adaptive value as it prepares to deal with threatening conditions. The almost immediate release of norepinephrine (NE) in the brain during emotional arousal binds to alpha and beta-adrenergic receptors (1). Tens of minutes later, the release of glucocorticoid hormones (GCs) peaks, driving many acute adaptations to stress through actions at glucocorticoid receptors (GRs) [for a review, (2)]. A seminal study showed that elevated corticosterone (CORT; the principal GC in rodents) levels enhance memory retention in tasks with high arousal content (3). The authors also demonstrated that arousal is determined by the NE levels that reach the amygdala's basolateral complex (BLA) (3).

However, maladaptation can sometimes follow stressor exposure (4). Exacerbated fear responses to stimuli that would not usually elicit such a response, avoidance behavior, and persistent anxiety symptoms are characteristic of anxiety- and stress-related disorders, such as generalized anxiety disorder and post-traumatic stress disorder (PTSD) (5). The relationship between an acute stressor and the delayed manifestation of anxiety symptoms has been widely studied, mainly because it resembles stress-related psychiatric disorders like PTSD.

Several studies have shown that a single two-hour stress session can produce anxiety-like behavior ten days later (6-9). In addition to promoting delayed anxiety-related behavior in rats, two-hour restraint stress and single prolonged stress protocols are associated with deficits in fear extinction memory (10, 11). Some studies have shown that acute two-hour immobilization stress or systemic CORT elevation promotes anxiety-like behavior in rats 10-12 days later, accompanied by increased spine density and dendritic arborization in the BLA (7, 12, 13). This delayed effect of stress on behavior is associated with morphological changes in the BLA, suggesting that increased synaptic contacts in this brain area are the basis for the increased anxiogenic drive. Thus, since hyperexcitability of the amygdala has also been linked to anxiety (14), it is plausible that BLA dendritic tree hypertrophy plays a causal role in anxiety.

Although there is a clear relationship between a transient increase in CORT levels and emergent anxiety-related behavior, it is unclear whether CORT acts directly on BLA neurons contributing to the behavioral and morphological effects after an acute stress episode. It also remains to be clarified whether these morphological changes in the BLA are sufficient to

83 promote anxiety or if there is a dependence on another mediator, in addition to CORT, for the
84 delayed behavioral manifestation associated with acute stress. Thus, the present study
85 sought to evaluate the role of GR, particularly the genomic actions of this receptor, in the BLA
86 at the time of stress in stress-induced behavioral and morphological outcomes. Considering
87 the pivotal participation of NE in modulating emotional arousal and neuronal excitability
88 (15), we also explored the role of BLA adrenergic receptors during stress-induced anxiety-
89 related behavior development.
90
91 **Results**
92
93 **Systemic CORT release is necessary for the delayed stress-induced anxiety-like**
94 **behavior and increased BLA dendritic spine density.**
95 To confirm whether the acute elevation of CORT plasma levels is essential to the
96 stress-related behavioral and neuroplastic effects, we inhibited the stress-induced rise in this
97 hormone's blood levels by administering metyrapone (Met). This compound inhibits the
98 synthesis of GCs, before stress exposure. The behavioral outcomes were then assessed ten
99 days later (Fig. 1A). As shown in Fig. 1B, pre-stress Met administration effectively prevented
100 the acute stress-induced increase in CORT plasma levels measured immediately after stress
101 exposure. In contrast, stressed animals administered saline presented higher plasma CORT
102 concentrations than non-stressed animals ($P < 0.001$) and stressed animals treated with Met
103 ($P < 0.001$).
104 Ten days after restraint stress, we assessed the anxiety-like behavior using the
105 elevated plus-maze (EPM) test. Like the previous results, pre-stress Met administration
106 blunted the acute stress-induced anxiety-like behavior onset and development. Indeed, Met-
107 administered stressed animals presented higher open arm exploration than saline-treated
108 stressed animals ($P < 0.01$, Fig. 1C; $P < 0.05$, Fig. 1D) and the same exploration profile as the
109 saline non-stressed animals (Fig. 1C and D). The anxiety index confirmed these data, being
110 higher in saline-treated stressed animals than in non-stressed ($P < 0.01$) and Met-treated
111 stressed animals ($P < 0.01$) (Fig. 1E). Finally, neither stress nor Met treatment influenced the
112 animals' motor behavior, as indicated by their total displacement in the maze (Fig. 1F and G).
113 We analyzed the effects of pre-stress Met administration on the delayed stress-
114 induced increase in dendritic spine density in the BLA using Golgi staining in a subset of the

115 rats that underwent behavioral evaluation (n = 4/group). We confirmed that a single two-
116 hour restraint stress exposure augmented the spine density in the primary ($P < 0.001$, Fig.
117 2A), secondary ($P < 0.001$, Fig. 2B), tertiary ($P < 0.001$, Fig. 2C), and quaternary ($P < 0.01$, Fig.
118 2D) segments of the BLA dendritic neurons compared to the non-stressed animals. Met
119 administration blunted the stress-induced increase in dendritic spine density in the BLA with
120 no effects in any dendritic segments of non-stressed animals (Fig. 2). These results suggest a
121 coordinated role of stress-induced systemic CORT elevation at the time of stress exposure in
122 the late development of anxiety-like behavior and BLA neuroplasticity.
123
124 **The delayed effects of acute stress on anxiety-like behavior and BLA dendritic spine**
125 **density increase depend on neuronal GR genomic activity.**
126 Next, we examined whether neuronal GR activation in the BLA was implicated in the
127 late stress outcomes associated with acute stress-induced plasma CORT elevation. Two hours
128 of restraint stress increased GR nuclear translocation into BLA neurons immediately after
129 stress (Fig. S1A and B). Moreover, Western blot analyses revealed an increase in GR nuclear
130 translocation in the BLA ($P = 0.0346$; Fig. S1C) and phosphorylation at the Ser211 site ($P =$
131 0.0166; Fig. S1D), which is associated with a gain in GR transcriptional function (16, 17). Ten
132 days after stress and immediately after the EPM test, there was no difference in the GR
133 nuclear translocation in the BLA of the stressed animals (Fig. S2). Likewise, we found no
134 changes in serum CORT levels of animals submitted to EPM previously stressed ten days
135 before, a result consistent with a previous study (8).
136 These findings collectively suggest that CORT signaling through GR at the time of
137 stress ultimately triggers delayed BLA alterations. In line with this, animals infused with the
138 GR antagonist RU486 directly into the BLA immediately before stress (Fig. S3A) displayed a
139 higher percentage of entries ($P = 0.0161$, Fig. S3B) and time spent ($P = 0.0215$; Fig. S3C) in
140 the EPM open arms ten days later, with no changes in the total distance traveled (Fig. S3D),
141 compared to stressed animals that received vehicle infusions.
142 Previous studies reported that a rise in CORT serum levels leads, via GR, to rapid
143 (non-genomic) and long-lasting (genomic) modifications in BLA neuronal excitability and
144 synaptic plasticity (18, 19). Because of the delayed effect of stress-associated GR signaling on
145 anxiety-like behavior and remodeling of dendritic spines in the BLA, we expressed a
146 transcriptionally inactive, truncated form of GR in the BLA, the so-called dominant negative

147 GR (dnGR). Cultured cells infected with dnGR responded to CORT treatment with the
148 receptor's translocation to the cell nucleus as control GFP-infected cells (Fig. S4A and B).
149 However, even with a high GR expression in the nucleus, dnGR-infected cells expressed fewer
150 GR-related mRNA transcription products than GFP-infected cells (Fig. S4C).

151 The HSV-based plasmid has a transgene expression peak three to four days after
152 infection, followed by a rapid decline in transgene expression (20). Thus, we exposed the
153 animals to restraint stress four to five days after intra-cranial delivery of the virus (Fig. 3A)
154 to maximize any inhibition of genomic GR activity during the stress session. The behavioral
155 test was administered ten days later, a time point at which viral expression of the transgene
156 should be minimal.

157 Stressed GFP-infected animals exhibited anxiety-like behavior, as evidenced by
158 reduced entries ($P < 0.01$; Fig. 3B) and time spent ($P < 0.01$; Fig. 3C) in open arms compared
159 to the GFP-infected non-stressed animals. On the other hand, dnGR expression in the BLA
160 prevented the anxiogenic effect of acute stress. Even when stressed, these animals displayed
161 similar levels of open arm exploration compared to the non-stressed GFP-infected group and
162 significantly increased open arm exploration relative to the stressed GFP-infected animals.
163 This situation was observed for open arm entries ($P < 0.05$) and the anxiety index ($P < 0.05$)
164 (Fig. 3B and D). There were no effects of stress or dnGR expression on distance traveled in
165 the maze, suggesting that differences in motor activity did not contribute to the observed
166 behavioral differences (Fig. 3E and F). Additionally, dnGR expression did not impact the
167 release of CORT during acute stress. Similar stress-induced levels of CORT were observed in
168 the stressed dnGR- and GFP-infected groups (Fig 3G) ($P < 0.001$ and $P < 0.01$, respectively).
169 Thus, the blunting of the delayed behavioral consequences of stress by dnGR is not due to
170 altered CORT release.

171 We measured the GFP protein signal throughout all subcellular compartments in
172 brain sections taken from the animals after the EPM and analyzed spine density to determine
173 whether dnGR expression prevented stress-induced changes in BLA spine density. As shown
174 in Fig. 4, there was a stress-induced increase in the dendritic spine density in the primary (P
175 < 0.05; Fig. 4A), secondary ($P < 0.05$; Fig. 4B), and tertiary ($P < 0.001$; Fig. 4C) dendritic
176 segments of GFP-infected animals compared to non-stressed animals. Interestingly, the
177 overexpression of dnGR in the BLA prevented the stress-induced increase in the spine

178 densities in the secondary ($P < 0.05$; Fig. 4B) and tertiary ($P < 0.001$; Fig. 4C) dendritic
179 segments but not in the primary ones (Fig. 4A).
180
181 **An increase in GR activity in the BLA is sufficient to induce a delayed anxiogenic effect.**
182 We stereotaxically injected dexamethasone (Dex) into the BLA. Ten days later, we
183 evaluated the anxiety-related behavior (Fig. 5A) to assess whether acute elevation of CORT
184 in the BLA was sufficient to induce delayed anxiety. The EPM test results showed that Dex
185 infusion attenuated the open-arm entry percentage ($P = 0.0482$; Fig. 5B) and time spent in
186 the open arms ($P = 0.0285$; Fig. 5C), and elevated anxiety index ($P = 0.0127$; Fig. 5D),
187 compared to stressed saline-infused animals. Since the Dex-treated animals moved less in the
188 maze than the saline ones ($P = 0.0048$; Fig. 5E and F), we performed a second anxiety-related
189 behavioral test, the light/dark box test. Since Dex-treated animals spent less time in the light
190 compartment than saline-administered animals, this test confirmed that Dex-treated animals
191 displayed more remarkable anxiety-like behavior than saline-treated animals ($P = 0.0369$;
192 Fig. 5G).
193
194 **BLA beta-adrenergic receptor activation is necessary for the expression of delayed**
195 **stress-related anxiety-like behavior.**
196 The acute anxiogenic effect of NE is widely known and involves the noradrenergic
197 projections from the locus coeruleus (LC) to the BLA (21). However, whether NE contributes
198 to delayed anxiogenic effects is not known. We addressed this question by infusing the alpha-
199 2 adrenergic receptor antagonist yohimbine into the BLA and examining the acute and
200 delayed effects on anxiety-like behavior (Fig. 6A). Previous studies reported that
201 antagonizing alpha-2 autoreceptors in the BLA increased firing from noradrenergic nerve
202 terminals (12, 13). Consistent with previous reports, we observed that increased NE activity
203 in the BLA produced an acute anxiogenic effect in the open field test (Fig 6B, C, D, E).
204 Additionally, intra-BLA administration of yohimbine did not induce anxiety-like behavior in
205 the EPM test ten days later (Fig. 6F, G, H, I).
206 Because increasing NE activity in the BLA has an acute, but not delayed, anxiogenic
207 effect, we examined whether beta-adrenergic receptor activity is critical for the delayed
208 manifestation of anxiety-like behavior in previously stressed animals. Thus, we administered
209 saline or propranolol, a beta-adrenoceptor antagonist, into the BLA of the animals before the

210 behavioral test, ten days after stress (Fig. 7A). As shown in Fig. 7, stressed propranolol-
211 treated animals presented a higher percentage of open arm entries ($P < 0.05$; Fig. 7B) and
212 time spent in the EPM ($P < 0.05$; Fig. 7C) than stressed saline-administered animals. These
213 effects were not accompanied by changes in the animals' locomotor activity (Fig. 7D).
214 Therefore, these results suggest that even at a delayed time point at which stress-dependent
215 increases in spine density are present (Fig. 2), stress-related changes in anxiety still depend
216 on beta-receptor activation in the BLA during the behavioral task.
217
218 **Discussion**
219 Here, we report that inhibiting CORT synthesis during acute stress prevented stress-
220 related behavioral and morphological effects that emerged ten days later. This finding
221 complements a previous study reporting that single systemic administration of CORT,
222 simulating an acute stress exposure, induced a delayed anxiogenic effect, along with parallel
223 increases in dendritic length, branch points, and spine density in BLA neurons (12, 13). It is
224 important to note that we showed that inhibiting CORT alone (Fig. 1-2), but not
225 catecholamines (Fig. 7, 6), sufficiently hindered these stress effects. In this sense, CORT
226 release is essential for the late effects of stress on anxiety-like behavior and dendritic
227 remodeling of the BLA, a result consistent with others (12, 22).
228 Amygdala hyperactivity is considered a biological substrate of stress- and anxiety-
229 related disorders in human and animal models (23). Stimulation of BLA projection neurons
230 triggers anxiety-like behavior in rodents (24), while acute and chronic stress increases the
231 intrinsic excitability of BLA pyramidal neurons (25, 26). Indeed, symptoms of anxiety
232 manifested by patients suffering from stress-related disorders, such as PTSD, are correlated
233 with amygdala hyperactivity (27, 28). The greater concentration of synaptic contacts in the
234 dendritic spines, compared to the rest of the neuronal surface, confers heightened ionic
235 conductance in this area, resulting in higher excitatory postsynaptic potentials (EPSPs)
236 amplitude (see (29). It is plausible that the delayed morphological changes in the BLA
237 dendritic tree following acute restraint stress produce a more excitable neuronal phenotype,
238 although this remains untested.
239 Accordingly, rats exposed to a single prolonged session of stress present the delayed
240 anxiogenic effect, which co-occurs with BLA dendritic tree hypertrophy and increased
241 miniature excitatory and inhibitory postsynaptic frequency currents in this brain area (30).

242 Interestingly, the lack of genomic GR signaling in the BLA neurons prevented the stress-
243 related increase in the spine density in the most distal dendritic branches (Fig. 4B, C) without
244 affecting the most proximal ones (Fig. 4A). This effect is consistent with other reports
245 showing that distal synaptic inputs on BLA neurons are more likely to be excitatory when
246 compared to proximal synapses, probably due to a higher GABAergic input in the latter (31).
247 A previous study reported that acute elevations in blood CORT levels modulate
248 dendritic spine turnover in the cortex, producing a short-term effect on eliminating and
249 forming new dendritic spines (32). Interestingly, acute stress and a single systematic
250 injection of CORT promote delayed (at least ten days later) but not short-term (one day later)
251 changes in the BLA dendritic tree (7, 22).
252 Protein synthesis is a critical step for forming new dendritic spines (33). Our findings
253 show that the stress-related anxiety-like behavior and the increase in the BLA dendritic spine
254 density are governed by the direct action of CORT in this brain region, phenomena dependent
255 on genomic GR activity. Notably, the GR mobilization by Dex injection into BLA generated a
256 delayed anxiety-like behavior even without stress. However, the mechanism by which GR
257 influences the origin and stabilization of new spines is not yet fully understood. Nevertheless,
258 growing evidence has shown a synergistic and interdependent action between GR and the
259 TRKB-BDNF receptor in the motor cortex during motor-related learning (34-36).
260 The role of NE in modulating behavior is well known and is closely related to the
261 immediate effects of changing/increasing the perception of threats during stress exposure
262 (37). Acute stress leads to a rapid release of NE in the limbic system, including the BLA and
263 hippocampus, primarily via projections of noradrenergic neurons from the LC (21, 38). The
264 activation of beta-adrenergic receptors in the BLA promotes increased excitatory synaptic
265 transmission and increased neuronal spike firing rates [see (15)]. In the present study, we
266 confirmed an acute anxiogenic effect of increased availability of NE in the BLA (via yohimbine
267 administration) (Fig. 6). Still, this increase in NE release did not promote delayed behavioral
268 changes. In contrast, Dex administration in the BLA was sufficient for promoting delayed
269 behavioral changes (Fig. 5). Additionally, blocking NE signaling directly into BLA with
270 propranolol at the time of behavioral testing prevented the manifestation of anxious-like
271 behavior in previously stressed animals (Fig. 7).
272 The synergism of GR and noradrenergic transmission in the BLA has already been
273 critical in potentiating the effects of arousal on memory retention (39). Here, we reported a

274 non-simultaneous but coordinated and (possibly) non-direct dependence of the delayed
275 manifestation of stress-induced anxiety on both GR and beta-adrenoceptor signaling in the
276 BLA. It is important to note that our previous study did not detect increased CORT release ten
277 days after the stress or immediately after the EPM test (8), indicating that elevated CORT
278 levels were not responsible for delayed anxiety-like behavior. We propose that the stress-
279 related delayed plastic changes in the BLA's dendritic arbor rely on genomic GR signaling
280 events, which may potentiate the stress response to NE. Therefore, given the morphological
281 effects of stress, the delayed behavioral outcome depends on NE signaling via beta-
282 adrenoceptors.
283
284 **Materials and Methods**
285
286 **Subjects**
287 Male Wistar rats (60-days old) were obtained from either the Facility for SPF Rat
288 Production at the Institute of Biomedical Sciences - Animal Facility Network at the University
289 of São Paulo (USP) or Harlan Sprague-Dawley Inc (Indianapolis, IN, USA). Neonatal Wistars
290 rats (1 - 4 days old) were used for the primary cortical culture. Upon arrival, the animals were
291 maintained at the vivarium in the USP Pharmacology Department (Unit 1) or Department of
292 Brain and Cognitive Sciences, Massachusetts Institute of Technology (MIT). The animals were
293 pair-housed in standard polypropylene cages (30 × 40 × 18 cm) with ad libitum access to food
294 and water in a temperature controlled (23 ± 2 ºC) room with a 12-hour light-dark cycle (light
295 on at 6:00 am). All experiments were conducted under the standards of the Ethics Committee
296 for Animal Use of the Institute of Biomedical Sciences/USP (CEUA - ICB 85/2016) and by the
297 Committee for Animal Care at MIT. All methods were in accordance with the Guidelines of the
298 Brazilian National Council for the Control of Animal Experimentation (CONCEA) and the US
299 National Institutes of Health (NIH) Guide for the Care and Use of Laboratory Animals.

300 Upon arrival in the vivarium, the animals were pair-housed in standard
301 polypropylene cages (30 × 40 × 18 cm), provided with food and water ad libitum, and
302 maintained in a temperature controlled (23 ± 2 ºC) room with a 12-hour light-dark cycle. All
303 experimental procedures were initiated after a habituation period of 7 to 10 days and
304 performed between 0900 and 1200 during the cycle's light phase.

305

306 **Animal experimental procedures**

307

308 ***Acute restraint stress***

309 The animals were placed in a ventilated PVC restraint tube for two hours in a lighted
310 and soundproof room. The behavioral experiments were conducted ten days after the end of
311 the stress session.

312

313 ***Behavioral tests***

314 The behavioral tests were conducted in a soundproof room with low light (10-14 lux).
315 All tests were videotaped using a digital video camera (Logitech C920, Lausanne,
316 Switzerland) from the top of the apparatuses. After each session, the apparatuses were
317 cleaned with 5% alcohol to remove olfactory cues.

318

319 *Elevated plus maze*

320 Animals were placed in the center of the maze (elevation of 50 cm, 50 cm × 10 cm
321 each arm), facing one of the open arms, and allowed to freely explore the apparatus for 5 min.
322 We scored entries, time spent in each arm, and the total displacement in the maze using
323 Ethovision software (Noldus, the Netherlands). The anxiety index (40, 41) was calculated as
324 follows: 1 - [(time spent in open arms/total time on the maze) + (number of entries to the
325 open arms/Total exploration in the maze)/2].

326

327 *Light/dark box*

328 Animals were placed in the middle of the light chamber (45 × 41 × 21 cm light
329 chamber, 65 lx; 35 × 41 × 21 cm dark chamber, 0 lx) facing the opposite side of the connecting
330 door. Each trial lasted 5 min, and the duration of time spent in the light chamber was used as
331 a parameter to address anxiety-like behavior.

332

333 ***Stereotactic surgery***

334 Drugs and viral vectors were injected into the BLA through stereotactic surgery, as
335 described by (42), with some modifications. Rats were anesthetized with isoflurane (4%
336 oxygen saturation for induction and 2-3% for maintenance), received a dose of anti-
337 inflammatory for preemptive analgesia (ketoprofen, 5 mg/kg, subcutaneous), and positioned
338 in the stereotaxic apparatus (Kopf Instruments). The skin was disinfected (70% ethanol, 1%
339 iodine, and 2% glycerin), the skin covering the skull was incised, and small holes were drilled
340 in the skull surface to pass cannulae or injection needles. The stainless-steel guide cannulae
341 (23-gauge, World Precision Instruments, Sarasota, FL, USA) were positioned bilaterally 1.0
342 mm dorsal to the BLA, using the following coordinates: A/P, -2.4; M/L, ± 5.1; D/V, -6.0 mm
343 relative to bregma and the surface of the brain (43). The cannulae were fixed with polyacrylic
344 cement and anchored to the skull with stainless steel screws. Drug infusions were made
345 through injectors (30-gauge stainless steel that extended 1.0 mm beyond the tip of each guide
346 cannula) after the animal's complete recovery from cannula implantation surgery (4 to 5
347 days). A polypropylene tube connected the injectors to a Hamilton syringe (5 µl, Hamilton
348 Co., Reno, NV, USA). The infusion rate was 0.1 µl/min with 1 min for diffusion before the
349 injector was removed from the guide cannula. The viral particles were injected with stainless-
350 steel needles coupled to a Hamilton syringe (5 µl, Hamilton Co.) fixed in an infusion pump
351 (Pump 11 Elite, Harvard Apparatus, Holliston, MA, USA) coupled to the stereotaxic apparatus.
352 The injections were placed bilaterally in the BLA using the following coordinates: A/P, -2.4;
353 M/L, ± 5.1; D/V, -7.0 mm. The viruses were infused at a rate of 0.1 µl/min for 20 min (total of
354 2 µl per injection site, totaling 2 × 106 viral particles). The needles remained in place for ten
355 minutes before being removed. The injections were performed 4-5 days before stress, a
356 critical time to reach the viral expression peak (44). Only animals with bilateral viral infection
357 in the BLA were considered in the behavioral analysis. After surgery, the animals were under
358 observation for three days. If they showed any sign of pain or discomfort, they received a
359 daily dose of anti-inflammatory (ketoprofen, 5 mg/kg, subcutaneous).

360

361 ***Cannula placement verification, viral infection visualization, and immunofluorescence***

362 Cannula placement verification was achieved by Nissl staining. The expression of GFP
363 indicated viral infection in the BLA. Animals in which the cannulae were not correctly
364 positioned bilaterally in the BLA, i.e., GFP expression was not restricted to the BLA, were

365 excluded from the study. The GFP detection and immunofluorescence assays are detailed
366 below.

367

368 ***Drug administration***

369 Metyrapone (i.p.; 150 mg in 1 ml of saline; Sigma-Aldrich) was administered 1.5 hours
370 before restraint stress. Bilateral intra-BLA infusion of RU-486 (10ng in 0.5 µl of 5% DMSO;
371 Sigma-Aldrich), dexamethasone (30 ng in 1 µl of 0.5% ethanol), propranolol (2.5 µg in 0.5 µl
372 of saline), or yohimbine (2.5 µg in 0.5 µl of saline), or their corresponding vehicle controls,
373 were performed via stereotaxic surgery.

374

375 **Viral vector construct**

376 Viral vectors containing the dnGR receptor gene sequence were constructed as
377 previously described (20, 45, 46). The dnGR gene construct is a chimera composed of the rat
378 GR alpha subunit (GenBank M14053), containing the ligand-binding domain, fused to the
379 human GR beta subunit (GenBank X03348), which includes the DNA-binding site domain. The
380 viral construct was obtained from the MIT viral core facility (McGovern Institute, MIT). The
381 dnGR was packaged in the HSV p1005 vector (short-term expression), a Herpes Simplex Virus
382 1 (HSV-1) derived amplicon plasmid with an added transcription cassette expressing GFP
383 (separate promoter and poly(A) (44, 47). The empty vector (lacking the dnGR sequence) was
384 used as a control. The IE 4/5 promoter drives the target gene, while a CMV promoter drives
385 the GFP gene. The two transcription cassettes are in a nose-to-tail orientation. Adherent 2-2
386 cells were transfected with the plasmid of interest (containing dnGR) using the Lipofectamine
387 LTX reagent (Invitrogen). Twenty-four hours after transfection, the cells were super-infected
388 with Helper Virus 5dl1.2, which has a multiplicity of infection of 0.03. The cells and media
389 were harvested 48 hours later when the virus's cytopathic effect reached 100%. The
390 solutions were frozen and thawed three times, sonicated to release infectious viral particles,
391 and then centrifuged to clear the media of cell debris. The resulting supernatant was passed
392 onto 2-2 cells. This amplification procedure was repeated twice. After the final sonication and
393 centrifugation, the supernatant was purified on a sucrose gradient, viral bands were
394 centrifuged, and viral pellets were resuspended in 10% sucrose in D-PBST. The vectors'

395 titration was quantified in Vero cells by counting the cells that express the GFP protein. An
396 average titration of approximately 1 × 106 viral particles per µl was achieved.
397
398 **Dendritic spine density analysis**
399 For some experiments, the brains were prepared using the Rapid Golgi Kit (FD
400 NeuroTechnologies, Inc., Columbia, MD, USA) according to the manufacturer's instructions.
401 An immunohistochemistry assay was performed for other experiments to amplify the GFP
402 signal to analyze the dendritic spine density in the BLA neurons previously infected with the
403 HSV vector.
404
405 ***Golgi staining and spine density analysis/Dendritic spine density analysis***
406 Brains were incubated in an impregnation solution for 14 days, followed by
407 incubation in a cryoprotectant solution for 48 hours. Samples were coronally sliced (120 µm)
408 using a Leica CM3050-S cryostat (Leica Biosystems) and mounted on gelatin-coated slides.
409 Brain sections were dehydrated in ethanol, diaphonized in xylene, and coverslipped. The
410 whole BLA images were captured in a bright field with the slide scanner Zeiss Axio Scan.Z1
411 (Zeiss), using a 40× objective. A z-stack with a 410 nm step size was created, and the images
412 were analyzed with the ZEN 2 (Zeiss) software at 600× magnification. At least five neurons
413 per animal (four animals per group) were analyzed according to the following criteria: only
414 neurons with the soma wholly localized in the BLA, heavily impregnated, without truncated
415 dendrites. After neuronal soma identification, we classified each dendritic segment as
416 primary (originating from the soma), secondary (originating from the primary branch),
417 tertiary (originating from the secondary branch), or quaternary (originating from the tertiary
418 branch). Regardless of the morphologic classification, all protrusions originating from a
419 dendrite were considered spines. After we determined the origin and the end of each branch,
420 the dendritic branch length was calculated by the software.
421
422 ***Brain tissue processing for immunofluorescence and immunohistochemistry***
423 Brains were sectioned in a cryostat (Leica CM3050-S, Leica Biosystems, Wetzlar,
424 Germany) in a coronal plane (40-µm-thick) at -22 °C and stored in an anti-freeze solution
425 (0.05 M sodium phosphate buffer, 150 g of sucrose, and 300 ml of ethylene glycol) at -20 °C.

426 We performed an immunofluorescence assay to visualize GR expression in the BLA.
427 Brain slices were incubated in blocking solution (0.02 M potassium phosphate solution
428 containing 0.3% Triton X-100 and 1% bovine serum albumin) for 1 hour, followed by
429 incubation in blocking solution containing the primary antibody (rabbit anti-GR, dilution 1:
430 1000, Santa Cruz; mouse anti-MAP-2, dilution 1: 5000, Sigma-Aldrich) for 18 hours (4 °C).
431 The slices were then incubated for two hours (room temperature) in a 0.02 M potassium
432 phosphate solution containing the secondary donkey antibody conjugated to a fluorochrome
433 (AlexaFluor 594 anti-rabbit, dilution 1: 500 or AlexaFluor 488 anti-mouse, dilution 1: 500,
434 Thermo Fisher Scientific). Brain slices were mounted on positively charged slides
435 (Fisherbrand Superfroast Plus, Thermo Fisher Scientific) and covered with a coverslip using
436 Fluoromount-G as the mounting medium (SouthernBiotech, Birmingham, AL, USA). The
437 images were acquired in a confocal microscope (Nikon A1R +, Nikon Instruments Inc.,
438 Melville, NY, USA), sectioned in the Z plane at 0.6 μm.

439 Although the HSV vector carries the gene that encodes GFP, an
440 immunohistochemistry procedure was performed to intensify the signal and improve GFP
441 particle detection throughout the BLA dendritic tree. Brain slices were incubated in blocking
442 solution (0.02 M potassium phosphate solution containing 0.3% Triton X-100 and 3% normal
443 donkey serum) followed by incubation in blocking solution containing the primary antibody
444 anti-GFP raised in rabbit (dilution 1: 1000; Thermo Fisher Scientific) for 18 hours at 4 °C. The
445 slices were then incubated in a 0.02 M potassium phosphate solution containing a
446 biotinylated donkey antibody (dilution 1: 200; Vector) and 0.3% Triton X-100 for two hours
447 at room temperature. The antigen-antibody complex was visualized with the biotin-avidin
448 technique (Elite kit; Vector Laboratories, Burlingame, CA, USA) and 3,3'-diaminobenzidine
449 (DAB) as a chromogen through a peroxidase reaction composed of a 2.5% solution of nickel
450 sulfate and 0.003% hydrogen peroxide in 0.02 M potassium phosphate buffer. The sections
451 were mounted on gelatin-coated slides, air-dried, and dipped in a 0.05% aqueous solution of
452 osmium tetroxide for 20 seconds to enhance the labeling's visibility, dehydrated, transferred
453 into xylene, and coverslipped with DPX. Spine density was quantified under a bright field, as
454 detailed for the Golgi staining assay.

455

456 **Western Blot**

457 GR expression and its phosphorylated form were analyzed by western blot as
458 previously (41).
459

460 *Protein extraction*

461 Cytosolic and nuclear protein extracts were obtained using the Cel-LyticTM
462 NuCLEARTM Extraction Kit (Sigma-Aldrich). BLA tissues stored at -80 ºC were thawed and
463 mechanically homogenized with a conical plastic pestle (Thermo Fisher Scientific) in cold
464 lysis buffer (10 mM HEPES, pH 7.9, 10 mM KCl, 1.5 mM MgCl2, 0.5 mm PMSF, 1 mm DTT)
465 supplemented with protease and phosphatase inhibitors (Halt Protease Inhibitor Cocktail,
466 ThermoFisher Scientific), and centrifuged for 20 min at 11,000 × g at 4 °C. The supernatant
467 (cytosolic fraction) was collected in a tube and stored at -80 °C. The remaining pellets were
468 homogenized in extraction buffer (20 mM HEPES, pH 7.9, 300 mM NaCl, 1.5 mM MgCl2, 0.25
469 mM EDTA, 0.5 mM PMSF, 0.5 mM DTT 25% glycerol) supplemented with protease and
470 phosphatase inhibitors, kept on ice for 30 min, and centrifuged for 5 min at 20,000 × g at 4
471 °C. The resulting supernatants (nuclear proteins) were stored at -80 °C. Protein concentration
472 was determined using the Bradford method (Bio-Rad Laboratories, Hercules, CA, USA).

473

474 *Electrophoresis*

475 Protein samples (20 µg/lane) were size-separated in 10% SDS-PAGE gel (90 V) and
476 then blotted onto Immobilon® PVDF membrane (EMD Millipore Corporation). The
477 immunoblots were stained Ponceau to ensure equal protein loading (48). Blots were blocked
478 with 5% BSA diluted in TBS-T buffer (50 mM Tris-HCl, 150 mM NaCl, 0.1% Tween 20, pH 7.5)
479 for one hour at room temperature and subsequently incubated overnight at 4 °C with specific
480 primary antibodies: monoclonal rabbit anti-GR (dilution 1:1000, Santa Cruz) or polyclonal
481 rabbit anti-Ser211phospho-GR (dilution 1:1000, Cell Signaling). After incubation with the
482 primary antibodies, membranes were probed with a secondary antibody conjugated to
483 horseradish peroxidase (dilution of 1:2000, Kirkegaard & Perry Laboratories, Gaithersburg,
484 MD, USA) for two hours at room temperature. The blots were developed using the Luminata
485 Forte Western HRP substrate (Merck Millipore, Darmstadt, Germany), and the signals were
486 recorded with the ChemiDoc system (Bio-Rad Laboratories). Several exposure times were
487 performed to ensure the linearity of the band intensities. Each band's relative density was

488 normalized to the value of α-Tubulin (sc-5286, dilution: 1:20,000, Santa Cruz Biotechnology,
489 Dallas, TX, USA).

490

491 **Primary cortical cell culture**

492 Neonatal rats were sacrificed by decapitation 1-4 days post-natal. The frontal cortex
493 was dissected in sterile medium (Hank's buffer: 160 mM NaCl, 5.3 mM KCl, 0.44 KH2PO4, 0.33
494 mM Na2HPO4, 5.5 mM glucose, 4.0 mM NaHCO3) supplemented with antibiotics
495 (penicillin/streptomycin, Invitrogen), at pH 7.4. The isolated frontal cortex was maintained
496 in Hank's buffer containing 0.05% trypsin (Vitrocell, Campinas, SP, Brazil) and 0.001%
497 DNAse (Sigma-Aldrich) at 37 °C for 10 minutes. Then the samples were then transferred to
498 Dulbecco's Modified Eagle Medium culture medium (DMEN; Vitrocell) plus 10% fetal bovine
499 serum (FBS, Vitrocell) and 2 mM glutamine (Sigma-Aldrich), in which it was gently
500 mechanically grounded with the aid of a Pasteur pipette. The solution was filtered through a
501 70 μM membrane (Becton-Dickinson), and the cells were further cultured in a 24-well plate
502 and incubated at 37 °C with 5% CO2 in a humidified atmosphere (80% relative humidity).
503 Cells were cultured on borosilicate coverslips covered with poly-L-lysine (0.01%, Sigma-
504 Aldrich) in a 24-well plate. For the immunofluorescence assays, the cells were counted before
505 plating using the Trypan Blue exclusion method (Sigma-Aldrich) to calculate the number of
506 viral particles necessary for efficient infection. The cells were maintained in DMEN
507 supplemented with antibiotics and 10% FBS. The medium was changed on the second and
508 fifth days after culturing and maintained until the tenth day.

509

510 **Infection of cells by viral particles and analysis of sub-localization and genomic activity**
511 **of GR**

512 Culture cells were infected with the viral particles (HSV-dnGR and HSV-GFP, MOI of
513 1) diluted in culture medium (DMEN + 2% FBS) on the eighth culture day to check the
514 sublocalization of the dnGR receptor in the cell compartments in response to CORT. Forty-
515 eight hours later (i.e., the tenth day of culture), the cells were treated with 10 μM CORT in
516 culture medium (DMEN + 2% FBS) for one hour. Then, the medium was removed, and the
517 coverslips were washed with PBS and fixed with 4% formaldehyde (Amresco) for 20 minutes

518 at room temperature. After five washes with PBS, the cells adhered to the coverslips were
519 incubated in a blocking solution (5% donkey serum, 0.05% Triton X-100 in PBS) for two
520 hours at room temperature. Next, the cells were incubated in a blocking solution containing
521 the primary anti-GR antibody (1: 1000, Santa Cruz) for 24 hours and then, after washing with
522 PBS, incubated in PBS containing the secondary antibody (AlexaFluor 594, 1: 2000) and
523 0.05% Triton X-100 for two hours. Finally, the coverslips were incubated in DAPI solution (1:
524 100,000, Sigma-Aldrich; PBS with 0.05% Triton X-100) for 20 minutes, washed with PBS, and
525 mounted on slides in Fluoromount-G mounting medium (SouthernBiotech). The slides were
526 analyzed under a fluorescence microscope (Nikon Eclipse 80i; Nikon Instruments Inc).

527 The polymerase chain reaction (PCR) assay was performed to amplify the Gilz and Fkbp5
528 genes described below and analyze the genomic GR activity in dnGR-infected cells. The cells
529 were obtained using the same protocol for image analysis, but the cells were not cultured on
530 coverslips. Instead, at the end of the treatment with CORT, the cells were washed five times
531 with PBS and collected in TRIzol® (0.75 µl per sample; Thermo Fisher Scientific). RNA
532 extraction was performed following the manufacturer's instructions.

533

534 **Polymerase chain reaction (PCR)**

535 After solubilizing the cells in TRIzol®, 175 µl of chloroform were added to each
536 sample, followed by incubation at room temperature for three minutes. The samples were
537 centrifuged at 12000 × g for 15 minutes at 4 °C, forming three phases. The first phase
538 contained the total RNA and was transferred to another tube. Next, 5 µg of RNase-free
539 glycogen and 0.5 ml of isopropanol alcohol were added for RNA precipitation. The samples
540 were incubated at room temperature for 10 minutes and centrifuged at 12000 × g for 10
541 minutes at 4 °C. After discarding the supernatant, 1 ml of 75% ethanol was added to the
542 resulting pellet, followed by vigorous vortexing and centrifugation at 7500 × g for 5 minutes
543 at 4 °C. After discarding the supernatant, the pellet was dried at room temperature, diluted
544 in DEPC water (20 µl), and stored at -80 °C. Two µl of the RNA was used for
545 spectrophotometric quantification at 260 and 280 nm in a Synergy HT Multi-Mode Microplate
546 Reader (BioTek Instruments, Inc, Winooski, VT, USA).

547 The cDNA was obtained using the SuperScript III Reverse Transcriptase Kit (Thermo Fisher
548 Scientific) according to the manufacturer's instructions. For the reaction, 12 µl of final

549 solution were used, containing 5 µg of RNA, 1 µl of dNTPs (0.5 nM each), 1 µl of Random
550 Primer in sterile water. The samples were incubated for 5 minutes at 70 °C, and then 8 µl of
551 the Mix solution was added to the solution, resulting in a final volume of 20 µl. Samples were
552 incubated for 10 minutes at 25 °C, 42 °C for 70 minutes, and 70 °C for 15 minutes to denature
553 the enzyme.

554 For the amplification, 2 µl of the cDNA (20 ng / µl), 5 µl of Amp Buffer, 0.75 ul MgCl2,
555 0.5 µl of dNTPs, 1.5 µl of the forward primer, 1.5 µl of the reverse primer, 0.5 µl of Taq
556 Polymerase (Promega Co), and Milli-Q water (Merck Millipore) sufficient for 25 µl were
557 added to a microtube. The reaction conditions in the thermal cycler (LifeECO, Bulldog Bio,
558 Inc) were: 95 °C for 2 initial minutes, followed by 30 cycles at 95 °C for 1 minute, 55 °C for 30
559 seconds, and 72 °C for 1 minute. After the last cycle, the samples remained at 72 °C for 5
560 minutes. The product was separated using agarose gel electrophoresis (2%), stained with
561 BlueGreen (Thermo Fisher Scientific), and visualized with a ChemiDoc Imager equipped with
562 a UV transilluminator (Bio-Rad Laboratories, Inc). The sequences of the primers used are as
563 follows:

564 Gapdh: forward, 5'-GGTGTGAACGGATTTGGC-3'

565 reverse, 5'-CTGG-AAGATGGTGATGGGTT-3'

566 Gilz: forward, 5'-TGGGGCCTAGTAACACCAAG-3'

567 reverse, 5'-GAGCACACTGGCATCACATC-3'

568 Fkbp5: forward, 5'-GAACCCAATGCTGAGCTTATG-3'

569 reverse, 5'- ATGTACTTGCCTCCCTTGAAG-3'

570

571 **Euthanasia of the animals and obtaining the analyzed material**

572

573 ***Guillotine beheading, BLA dissection and blood collection***

574 The animals were deeply anesthetized with isoflurane (maximum exposure of 30 s)
575 and euthanatized by decapitation. The brain was quickly removed in a cold solution of saline-
576 phosphate buffer (137 mM NaCl, 2.68 mM KCl, 1.27 mM KH2PO4, 8.06 mM Na2HPO4). The
577 BLA was bilaterally dissected on a cold glass plate and frozen in a conical tube (1.5 ml) on dry

578 ice. The brain structures were stored at –80 ºC for later use. Brains were placed in a 1 mm
579 thick coronal cut acrylic brain matrix (Zivic Laboratories Inc., New Castle, PA, USA), and the
580 dissection was performed under a stereomicroscope (Tecnival – Prolab, Diadema, SP, Brazil).
581 Blood was obtained from the animals' trunks at the time of decapitation.

582

583 ***Transcardiac perfusion***

584 The animals were deeply anesthetized with a solution of ketamine hydrochloride (9
585 mg / 100 g, i.p.) and xylazine (1 mg / 100g, i.p.) and infused transcardiacally using a peristaltic
586 pump (Cole Parmer, Vernon Hills, IL, USA), with 200 ml of 0.9% saline followed by about 500
587 ml of 4% formaldehyde solution in sodium phosphate buffer (pH 7.4) at 4 °C for 20 minutes.
588 After three hours, the brain was removed from the skull and kept in a 30% sucrose solution
589 in potassium phosphate buffer (0.02 M) at 4 °C for 48 hours. After this cryoprotection period,
590 the brain was removed from the sucrose solution and frozen at -80 °C until histological
591 processing.

592

593 ***Blood collection and plasma obtaining***

594 Blood was sampled from the body trunk after decapitation, immediately after stress
595 termination. Plasma was obtained by adding EDTA (4.5 mM) to the collected blood and
596 centrifugation at 4000 × g for 10 minutes. Samples were stored at -80 ºC.

597

598 **Analysis of the concentration of corticosterone in the blood**

599 The Corticosterone EIA kit (Enzo Life Sciences, Inc, Farmingdale, NY, USA) was used
600 to analyze blood CORT levels, following the manufacturer's guidelines. Plasma samples were
601 diluted at 1:30 in the assay buffer provided by the kit to fit the standard curve's optimal range.
602 The values depicted in the figures were corrected for the dilution factor.

603

604 **Statistics**

605 Statistical analysis was performed using two-way ANOVA. Post hoc Tukey's multiple
606 comparison test examined differences between individual groups. An unpaired Student's t-

test was used to compare two experimental groups when appropriate. Sample size and animal numbers were estimated based on previous studies, and the ROUT method checked the outlier samples. Quantification of data was blind for all experiments. GraphPad Prism software 9.0 was used for the statistical analysis, and the level of statistical significance was $p < 0.05$. Data are presented as the mean ± SEM. Detailed statistical information for each test performed is reported in the figure legends.

Acknowledgments

We gratefully thank Guiomar Wiesel for her technical assistance. We dedicate this work to Dr. Nilton Barreto dos Santos, a superb young scientist and a dear friend, victim of COVID-19.

Funding

This work was supported by the Fundação de Amparo à Pesquisa do Estado de São Paulo (FAPESP 2016/03572-3 and 2019/00908-9) and Conselho Nacional de Desenvolvimento Científico e Tecnológico (CNPq 422523/2016-0) to CDM and a grant from the U.S. Army Research Office and the Defense Advanced Research Projects Agency (grant W911NF-10-1-0059) to KAG. L.S.N. was supported by FAPESP (2012/24002-0 and 2018/19599-3). L.M.B.C. was supported by CAPES, CNPq (142260/2019-3), and FAPESP (2018/15982-7). N.B.S. was supported by FAPESP (2018/17991-3). A.S.A. was supported by FAPESP (2019/00400-5) and CAPES. V.A.L.J. was supported by FAPESP (2020/06914-8) and CNPq (PIBIC 2019-1429). C.D.M. is research fellow from CNPq. This study was financed in part by the Coordenação de Aperfeiçoamento de Pessoal de Nível Superior - Brasil (CAPES) - Finance Code 001.

Competing Interest Statement

The authors declared no conflicts of interest concerning their authorship or the publication of this article.

Supplementary information is available.

References

636 1. H. J. Krugers, H. Karst, M. Joels, Interactions between noradrenaline and
637 corticosteroids in the brain: from electrical activity to cognitive performance. *Front*
638 *Cell Neurosci* **6**, 15 (2012).

639 2. E. R. de Kloet, M. Joels, F. Holsboer, Stress and the brain: from adaptation to disease.
640 *Nature reviews. Neuroscience* **6**, 463-475 (2005).

641 3. B. Roozendaal, S. Okuda, E. A. Van der Zee, J. L. McGaugh, Glucocorticoid enhancement
642 of memory requires arousal-induced noradrenergic activation in the basolateral
643 amygdala. *Proceedings of the National Academy of Sciences of the United States of*
644 *America* **103**, 6741-6746 (2006).

645 4. B. S. McEwen, H. Akil, Revisiting the Stress Concept: Implications for Affective
646 Disorders. *The Journal of neuroscience : the official journal of the Society for*
647 *Neuroscience* **40**, 12-21 (2020).

648 5. D. A. Regier, E. A. Kuhl, D. J. Kupfer, The DSM-5: Classification and criteria changes.
649 *World Psychiatry* **12**, 92-98 (2013).

650 6. P. Chakraborty, S. Datta, B. S. McEwen, S. Chattarji, Corticosterone after acute stress
651 prevents the delayed effects on the amygdala. *Neuropsychopharmacology : official*
652 *publication of the American College of Neuropsychopharmacology* **45**, 2139-2146
653 (2020).

654 7. R. Mitra, S. Jadhav, B. S. McEwen, A. Vyas, S. Chattarji, Stress duration modulates the
655 spatiotemporal patterns of spine formation in the basolateral amygdala. *Proceedings*
656 *of the National Academy of Sciences of the United States of America* **102**, 9371-9376
657 (2005).

658 8. L. S. Novaes, N. B. Dos Santos, J. G. Perfetto, K. A. Goosens, C. D. Munhoz, Environmental
659 enrichment prevents acute restraint stress-induced anxiety-related behavior but not
660 changes in basolateral amygdala spine density. *Psychoneuroendocrinology* **98**, 6-10
661 (2018).

662 9. F. Yasmin *et al.*, Stress-induced modulation of endocannabinoid signaling leads to
663 delayed strengthening of synaptic connectivity in the amygdala. *Proceedings of the*
664 *National Academy of Sciences of the United States of America* **117**, 650-655 (2020).

665 10. P. R. Abdullahi *et al.*, Protective effects of morphine in a rat model of post-traumatic
666 stress disorder: Role of hypothalamic-pituitary-adrenal axis and beta- adrenergic
667 system. *Behavioural brain research* **395**, 112867 (2020).

668 11. L. S. Novaes, L. M. Bueno-de-Camargo, C. D. Munhoz, Environmental enrichment
669 prevents the late effect of acute stress-induced fear extinction deficit: the role of
670 hippocampal AMPA-GluA1 phosphorylation. *Transl Psychiatry* **11**, 18 (2021).

671 12. R. Mitra, R. M. Sapolsky, Acute corticosterone treatment is sufficient to induce anxiety
672 and amygdaloid dendritic hypertrophy. *Proceedings of the National Academy of*
673 *Sciences of the United States of America* **105**, 5573-5578 (2008).

674 13. R. P. Rao, S. Anilkumar, B. S. McEwen, S. Chattarji, Glucocorticoids protect against the
675 delayed behavioral and cellular effects of acute stress on the amygdala. *Biological*
676 *psychiatry* **72**, 466-475 (2012).

677 14. N. Daviu, M. R. Bruchas, B. Moghaddam, C. Sandi, A. Beyeler, Neurobiological links
678 between stress and anxiety. *Neurobiol Stress* **11**, 100191 (2019).

679 15. A. E. Fink, J. E. LeDoux, beta-Adrenergic enhancement of neuronal excitability in the
680 lateral amygdala is developmentally gated. *J Neurophysiol* **119**, 1658-1664 (2018).

681 16. W. Chen *et al.*, Glucocorticoid receptor phosphorylation differentially affects target
682 gene expression. *Mol Endocrinol* **22**, 1754-1766 (2008).

683 17. M. D. Krstic, I. Rogatsky, K. R. Yamamoto, M. J. Garabedian, Mitogen-activated and
684 cyclin-dependent protein kinases selectively and differentially modulate
685 transcriptional enhancement by the glucocorticoid receptor. *Mol Cell Biol* **17**, 3947-
686 3954 (1997).

687 18. S. Duvarci, D. Pare, Glucocorticoids enhance the excitability of principal basolateral
688 amygdala neurons. *The Journal of neuroscience : the official journal of the Society for*
689 *Neuroscience* **27**, 4482-4491 (2007).

690 19. H. Karst, S. Berger, G. Erdmann, G. Schutz, M. Joels, Metaplasticity of amygdalar
691 responses to the stress hormone corticosterone. *Proceedings of the National Academy*
692 *of Sciences of the United States of America* **107**, 14449-14454 (2010).

693 20. D. Kaufer *et al.*, Restructuring the neuronal stress response with anti-glucocorticoid
694 gene delivery. *Nature neuroscience* **7**, 947-953 (2004).

695 21. J. G. McCall *et al.*, Locus coeruleus to basolateral amygdala noradrenergic projections
696 promote anxiety-like behavior. *Elife* **6** (2017).

697 22. H. Kim *et al.*, Regional differences in acute corticosterone-induced dendritic
698 remodeling in the rat brain and their behavioral consequences. *BMC Neurosci* **15**, 65
699 (2014).

700 23. B. M. Sharp, Basolateral amygdala and stress-induced hyperexcitability affect
701 motivated behaviors and addiction. *Transl Psychiatry* **7**, e1194 (2017).

702 24. G. G. Calhoon, K. M. Tye, Resolving the neural circuits of anxiety. *Nature neuroscience*
703 **18**, 1394-1404 (2015).

704 25. A. Hetzel, J. A. Rosenkranz, Distinct effects of repeated restraint stress on basolateral
705 amygdala neuronal membrane properties in resilient adolescent and adult rats.
706 *Neuropsychopharmacology : official publication of the American College of*
707 *Neuropsychopharmacology* **39**, 2114-2130 (2014).

708 26. J. A. Rosenkranz, E. R. Venheim, M. Padival, Chronic stress causes amygdala
709 hyperexcitability in rodents. *Biological psychiatry* **67**, 1128-1136 (2010).

710 27. A. M. Hull, Neuroimaging findings in post-traumatic stress disorder. Systematic
711 review. *Br J Psychiatry* **181**, 102-110 (2002).

712 28. R. K. Pitman *et al.*, Biological studies of post-traumatic stress disorder. *Nature reviews.*
713 *Neuroscience* **13**, 769-787 (2012).

714 29. A. T. Gulledge, N. T. Carnevale, G. J. Stuart, Electrical advantages of dendritic spines.
715 *PloS one* **7**, e36007 (2012).

716 30. H. H. Zhang *et al.*, Traumatic Stress Produces Delayed Alterations of Synaptic
717 Plasticity in Basolateral Amygdala. *Front Psychol* **10**, 2394 (2019).

718 31. P. M. Klenowski *et al.*, Structural and functional characterization of dendritic arbors
719 and GABAergic synaptic inputs on interneurons and principal cells in the rat
720 basolateral amygdala. *J Neurophysiol* **114**, 942-957 (2015).

721 32. C. Liston, W. B. Gan, Glucocorticoids are critical regulators of dendritic spine
722 development and plasticity in vivo. *Proceedings of the National Academy of Sciences of*
723 *the United States of America* **108**, 16074-16079 (2011).

724 33. J. Tanaka *et al.*, Protein synthesis and neurotrophin-dependent structural plasticity of
725 single dendritic spines. *Science* **319**, 1683-1687 (2008).

726 34. M. Arango-Lievano *et al.*, Persistence of learning-induced synapses depends on
727 neurotrophic priming of glucocorticoid receptors. *Proceedings of the National*
728 *Academy of Sciences of the United States of America* **116**, 13097-13106 (2019).

729 35. M. Arango-Lievano *et al.*, Neurotrophic-priming of glucocorticoid receptor signaling
730 is essential for neuronal plasticity to stress and antidepressant treatment.
731 *Proceedings of the National Academy of Sciences of the United States of America* **112**,
732 15737-15742 (2015).

733 36. F. Jeanneteau, M. J. Garabedian, M. V. Chao, Activation of Trk neurotrophin receptors
734 by glucocorticoids provides a neuroprotective effect. *Proceedings of the National*
735 *Academy of Sciences of the United States of America* **105**, 4862-4867 (2008).

736 37. G. Aston-Jones, J. Rajkowski, J. Cohen, Role of locus coeruleus in attention and
737 behavioral flexibility. *Biological psychiatry* **46**, 1309-1320 (1999).

738 38. R. J. Valentino, E. Van Bockstaele, Convergent regulation of locus coeruleus activity as
739 an adaptive response to stress. *European journal of pharmacology* **583**, 194-203
740 (2008).

741 39. D. de Quervain, L. Schwabe, B. Roozendaal, Stress, glucocorticoids and memory:
742 implications for treating fear-related disorders. *Nature reviews. Neuroscience* **18**, 7-
743 19 (2017).

744 40. H. Cohen, M. A. Matar, D. Buskila, Z. Kaplan, J. Zohar, Early post-stressor intervention
745 with high-dose corticosterone attenuates posttraumatic stress response in an animal
746 model of posttraumatic stress disorder. *Biological psychiatry* **64**, 708-717 (2008).

747 41. L. S. Novaes *et al.*, Environmental enrichment protects against stress-induced anxiety:
748 Role of glucocorticoid receptor, ERK, and CREB signaling in the basolateral amygdala.
749 *Neuropharmacology* **113**, 457-466 (2017).

750 42. L. S. Novaes, S. J. Shammah-Lagnado, Projections from the anteroventral part of the
751 medial amygdaloid nucleus in the rat. *Brain research* **1421**, 30-43 (2011).

752 43. G. Paxinos, C. Watson, *The Rat Brain in Stereotaxic Coordinates.* (Elsevier, London, ed.
753 6th Edition, 2007), pp. 476.

754 44. S. J. Russo *et al.*, Nuclear factor kappa B signaling regulates neuronal morphology and
755 cocaine reward. *The Journal of neuroscience : the official journal of the Society for*
756 *Neuroscience* **29**, 3529-3537 (2009).

757 45. E. D. Kirby *et al.*, Basolateral amygdala regulation of adult hippocampal neurogenesis
758 and fear-related activation of newborn neurons. *Molecular psychiatry* **17**, 527-536
759 (2012).

760 46. R. M. Meyer, A. Burgos-Robles, E. Liu, S. S. Correia, K. A. Goosens, A ghrelin-growth
761 hormone axis drives stress-induced vulnerability to enhanced fear. *Molecular*
762 *psychiatry* **19**, 1284-1294 (2014).

763 47. R. L. Neve, F. Lim, Generation of high-titer defective HSV-1 vectors. *Current protocols*
764 *in neuroscience / editorial board, Jacqueline N. Crawley ... [et al.]* **Chapter 4**, Unit 4 13
765 (2013).

766 48. O. Salinovich, R. C. Montelaro, Reversible staining and peptide mapping of proteins
767 transferred to nitrocellulose after separation by sodium dodecylsulfate-
768 polyacrylamide gel electrophoresis. *Analytical biochemistry* **156**, 341-347 (1986).

769 **Figures and Tables**
770

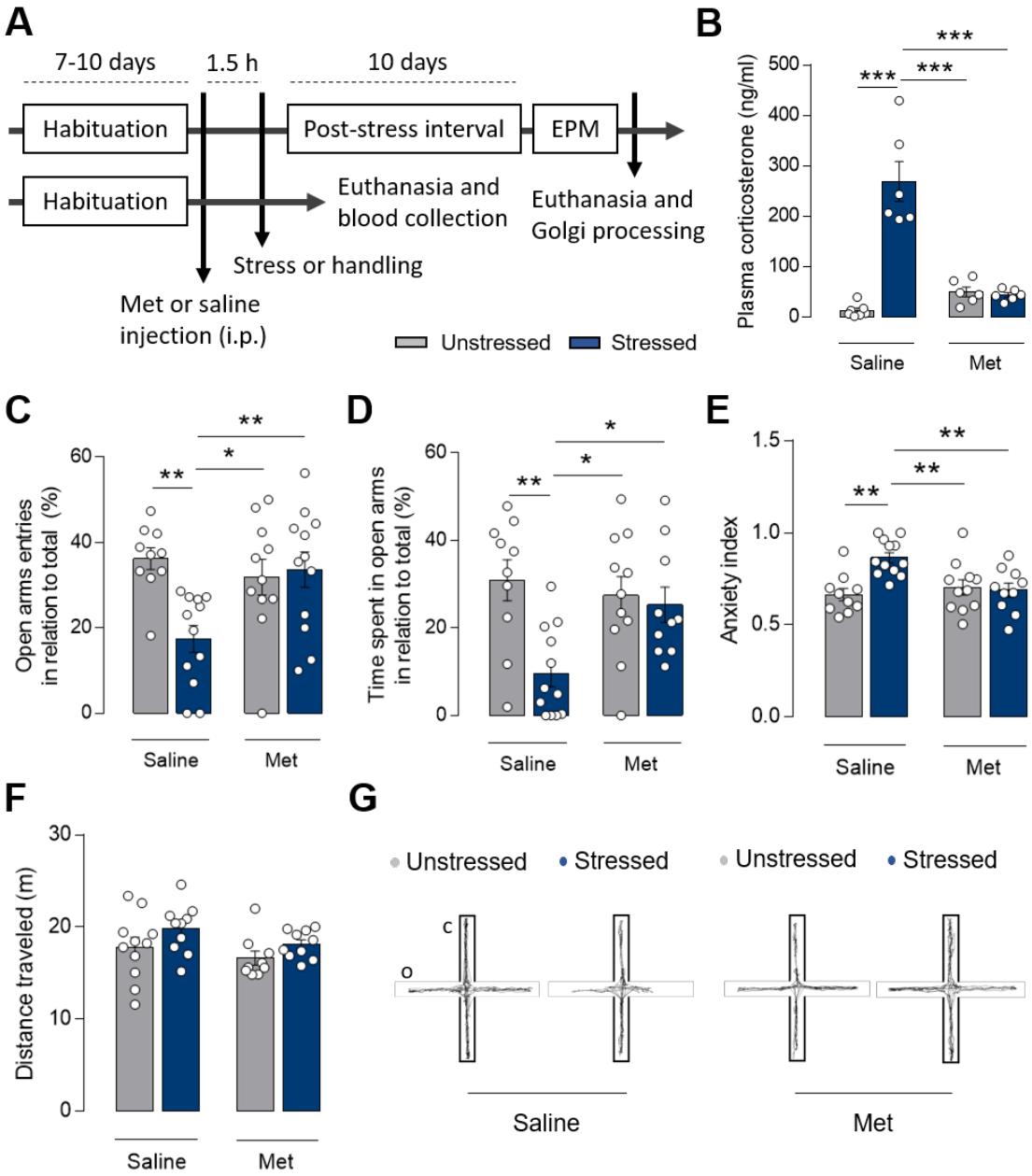

771
772

773 **Figure 1.** CORT synthesis inhibition during stress prevented the delayed emergence of
774 anxiety-like behavior. (A) Schematic representation of the experimental design showing the
775 timeline of vehicle (saline) or metyrapone (Met) injections, the stress submission, and the
776 EPM behavioral test. One cohort of animals was euthanized immediately after the end of the
777 stress session. (B) Previous administration of Met prevented the stress-induced increase in
778 CORT plasma levels measured immediately after stress (n = 6–7 animals for each group, two-
779 way ANOVA: stress $F_{1, 21} = 40.34$, $P < 0.0001$; Met $F_{1, 21} = 22.81$, $P = 0.0001$; stress-Met

interaction $F_{1, 21} = 44.35$, $P < 0.0001$). (C and D) Stressed animals treated with saline exhibited reduced open arm entries and time spent in the EPM test compared to saline-treated non-stressed animals and stressed and non-stressed Met-treated animals (C; n = 10–12 animals for each group, two-way ANOVA: stress $F_{1, 40} = 4.692$, $P = 0.0363$; Met $F_{1, 40} = 3.23$, $P = 0.0799$; stress-Met interaction $F_{1, 40} = 8.9$, $P = 0.0048$; D; n = 10–12 animals for each group, two-way ANOVA: stress $F_{1, 39} = 8.712$, $P = 0.0053$; Met $F_{1, 39} = 5.783$, $P = 0.0210$; stress-Met interaction $F_{1, 39} = 2.352$, $P = 0.1332$). (E) Stress increased the anxiety index in saline-treated but not in Met-treated rats (n = 10–12 animals for each group, two-way ANOVA: stress $F_{1, 39} = 6.85$, $P = 0.0126$; Met $F_{1, 39} = 3.786$, $P = 0.0589$; stress-Met interaction $F_{1, 39} = 9.282$, $P = 0.0041$). (F) Neither stress nor Met administration influenced the animal's locomotor activity in the EPM (n = 9–12 animals for each group, two-way ANOVA: stress $F_{1, 34} = 2.388$, $P = 0.1315$; Met $F_{1, 34} = 3.78$, $P = 0.0602$; stress-Met interaction $F_{1, 34} = 0.1839$, $P = 0.6707$). (G) Representative tracking plots for the average motion of each experimental group in the EPM. Results are represented as the mean ± SEM. Tukey's multiple comparisons post-hoc test. Significance differences between groups are indicated as * $P < 0.05$; ** $P < 0.01$; and *** $P < 0.001$.

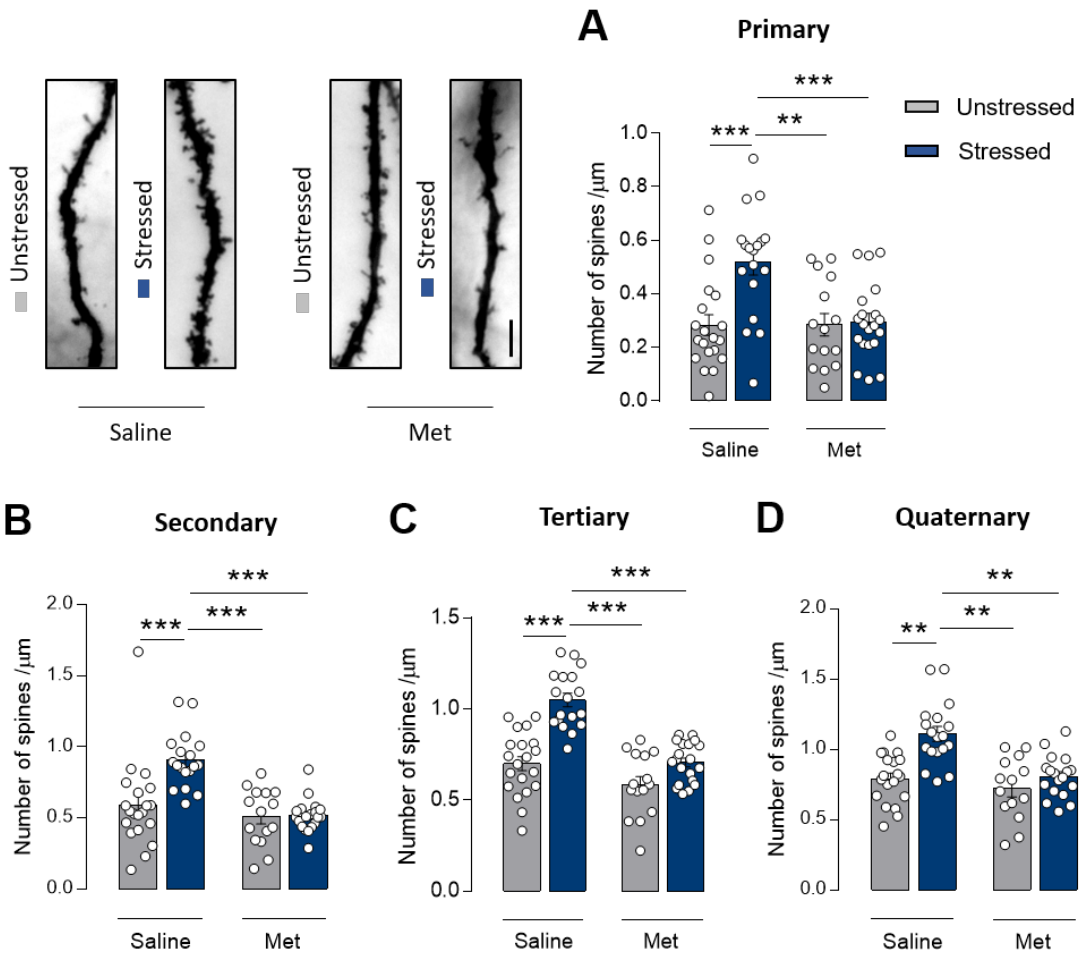

Figure 2. Pre-stress Met administration prevented the stress-induced increase in BLA dendritic spine density. (A-D) Stressed saline-treated animals showed an increase in spine density, an effect prevented by pre-stress Met administration in the primary (A; n = 15–20 neurons for each group, two-way ANOVA: stress F1, 69 = 9.351, P = 0.0032; Met F1, 69 = 7.786, P = 0.0079; stress-Met interaction F1, 69 = 7.72, P = 0.0070), secondary (B; n = 15–20 neurons for each group, two-way ANOVA: stress F1, 69 = 9.871, P = 0.0025; Met F1, 69 = 20.65, P < 0.0001; stress-Met interaction F1, 69 = 8.895, P = 0.0038), tertiary (C; n = 15–20 neurons for each group, two-way ANOVA: stress F1, 69 = 42.17, P < 0.0001; Met F1, 69 = 39.75, P < 0.0001; stress-Met interaction F1, 69 = 9.809, P = 0.0025), and quaternary (D; n = 14–20 neurons for each group, two-way ANOVA: stress F1, 65 = 18.62, P < 0.0001; Met F1, 65 = 15.92, P = 0.0002; stress-Met interaction F1, 65 = 6.267, P = 0.0148) dendrite segments compared to non-stressed animals. (Top, left) Representative photomicrography of a BLA's secondary dendrite segment. (Scale bar, 10 µm). Results are represented as the mean ± SEM. Tukey's multiple comparisons post-hoc test). Significant differences between groups are indicated as ** P < 0.01 and *** P < 0.001.

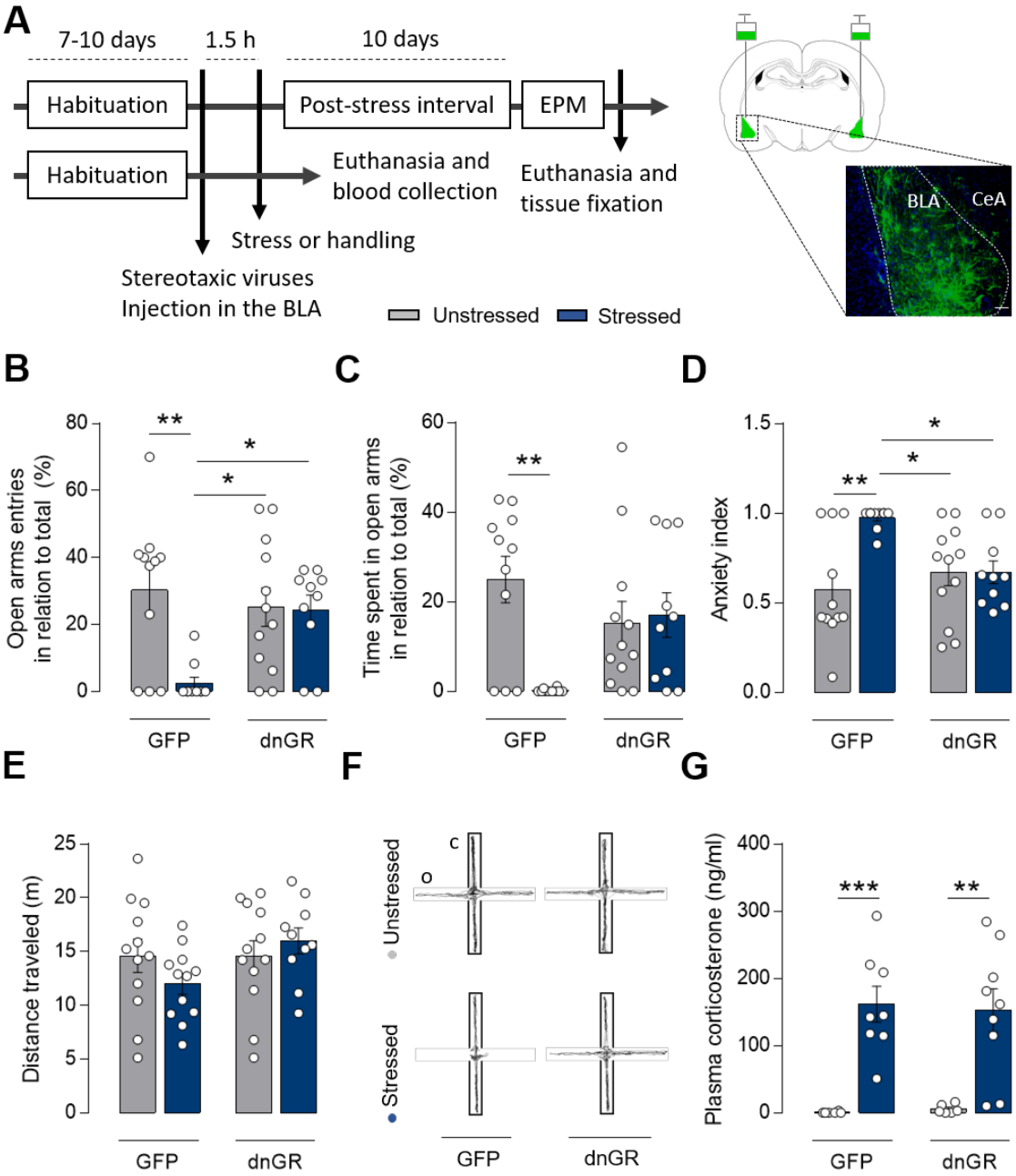

Figure 3. dnGR overexpression in the BLA prevented the delayed emergence of stress-induced anxiety-like behavior. (A, left) Schematic representation of the experimental design shows the virus injection timeline into BLA (GFP or dnGR), the stress submission, and the EPM behavioral test. A cohort of animals was euthanized immediately after the end of the stress session. (Right) Representative figure showing the viral injection into BLA and photomicrography of an infected BLA (GFP, green). (Scale bar, 100 µm). CeA: central nucleus of the amygdala. (B) GFP-stressed animals exhibited reduced open arm entries in the EPM

827 test compared to GFP-non-stressed and stressed and non-stressed animals overexpressing
828 dnGR in the BLA (n = 10–12 animals for each group, two-way ANOVA: stress $F_{1, 39} = 7.527$,
829 $P = 0.0091$; dnGR $F_{1, 39} = 2.612$, $P = 0.1114$; stress-dnGR interaction $F_{1, 39} = 6.724$, $P =$
830 0.0133). (C) GFP-stressed animals spent less time in the EPM open arms than GFP-non-
831 stressed animals. dnGR animals (stressed and non-stressed) exhibited no differences in time
832 spent in open arms compared to GFP non-stressed animals (n = 10–12 animals for each
833 group, two-way ANOVA: stress $F_{1, 39} = 6.595$, $P = 0.0142$; dnGR $F_{1, 39} = 0.6368$, $P = 0.4297$;
834 stress-dnGR interaction $F_{1, 39} = 8.864$, $P = 0.0050$). (D) Stress increased the anxiety index in
835 GFP-expressing but not in dnGR-expressing rats (n = 10–12 animals for each group, two-way
836 ANOVA: stress $F_{1, 39} = 7.943$, $P = 0.0075$; dnGR $F_{1, 39} = 2.06$, $P = 0.1592$; stress-dnGR
837 interaction $F_{1, 39} = 8.047$, $P = 0.0072$). (E) Neither stress nor BLA virus infection influenced
838 the animal's locomotor activity in the EPM (n = 10–12 animals for each group, two-way
839 ANOVA: stress $F_{1, 42} = 0.212$, $P = 0.6476$; dnGR $F_{1, 42} = 2.257$, $P = 0.1405$; stress-dnGR
840 interaction $F_{1, 42} = 2.283$, $P = 0.1383$). (F) Representative tracking plots for the average
841 motion of each experimental group in the EPM. (G) Acute restraint stress increases CORT
842 plasma levels in GFP- and dnGR-overexpressing animals immediately after the stressor
843 stimulus (n = 6–9 animals for each group, two-way ANOVA: stress $F_{1, 25} = 36.25$, $P < 0.0001$;
844 dnGR $F_{1, 25} = 0.007222$, $P = 0.9330$; stress-dnGR interaction $F_{1, 25} = 0{,}07801$, $P = 0.7823$).
845 Results are represented as the mean ± SEM. Tukey's multiple comparisons post-hoc test.
846 Significant differences between groups are indicated as * $P < 0.05$, ** $P < 0.01$, and *** $P <$
847 0.001.
848
849

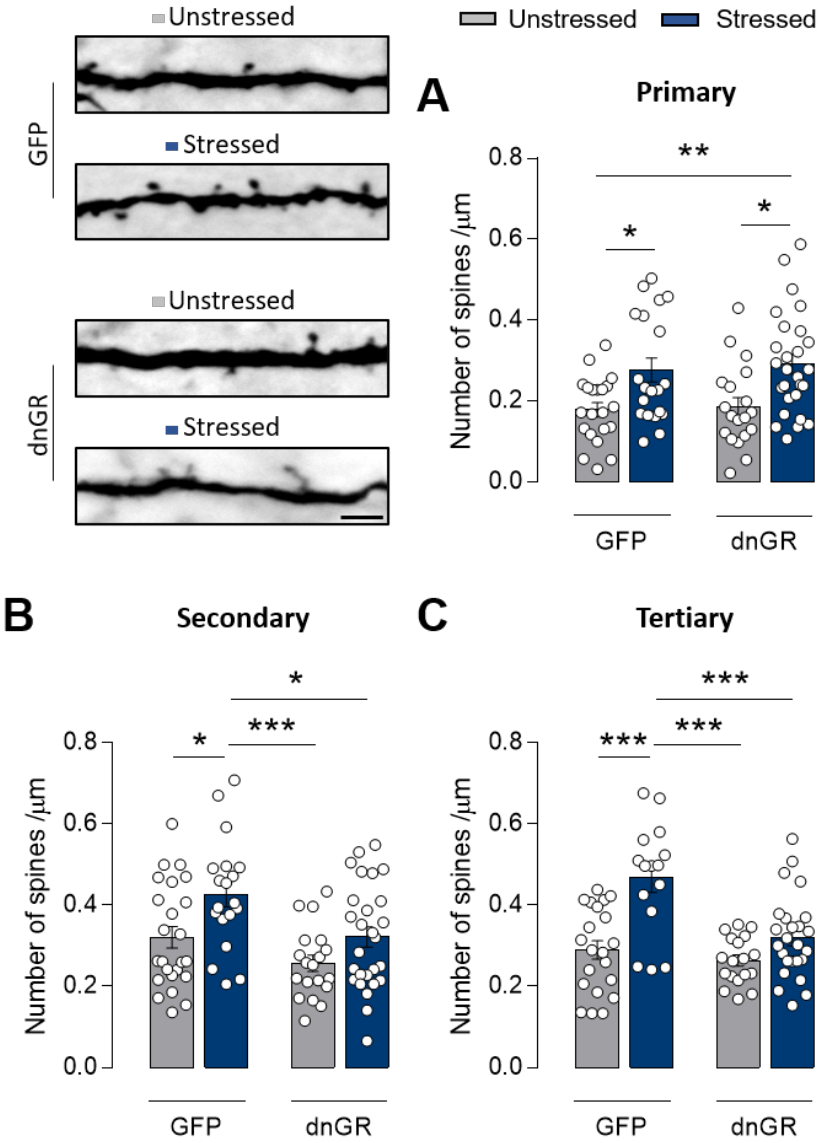

Figure 4. dnGR expression in the BLA prevented the stress-related increase in BLA's dendritic spine density. (A-C) GFP-stressed animals showed an increase in spine density, an effect prevented by the dnGR overexpressing in the BLA in the primary (A; n = 19–27 neurons for each group, two-way ANOVA: stress $F_{1, 83} = 17.32$, $P < 0.0001$; dnGR $F_{1, 83} = 0.188$, $P = 0.6657$; stress-dnGR interaction $F_{1, 83} = 0.02408$, $P = 0.8771$), secondary (B; n = 19–27 neurons for each group, two-way ANOVA: stress $F_{1, 85} = 10.49$, $P = 0.0017$; dnGR $F_{1, 85} = 10.34$, $P = 0.0018$; stress-dnGR interaction $F_{1, 85} = 0.6021$, $P = 0.4399$), and tertiary (C; n = 15–25 neurons for each group, two-way ANOVA: stress $F_{1, 69} = 16.8$, $P = 0.0001$; dnGR $F_{1, 69} = 8.421$, $P = 0.0050$; stress-dnGR interaction $F_{1, 69} = 7.85$, $P = 0.0066$) dendrite segments compared to non-stressed animals. (Top, left) Representative photomicrography of a BLA's secondary dendrite segment. (Scale bar, 10 µm). Results are represented as the mean ± SEM. Tukey's multiple comparisons post-hoc test. Significant differences between groups are indicated as * $P < 0.05$, ** $P < 0.01$, and *** $P < 0.001$.

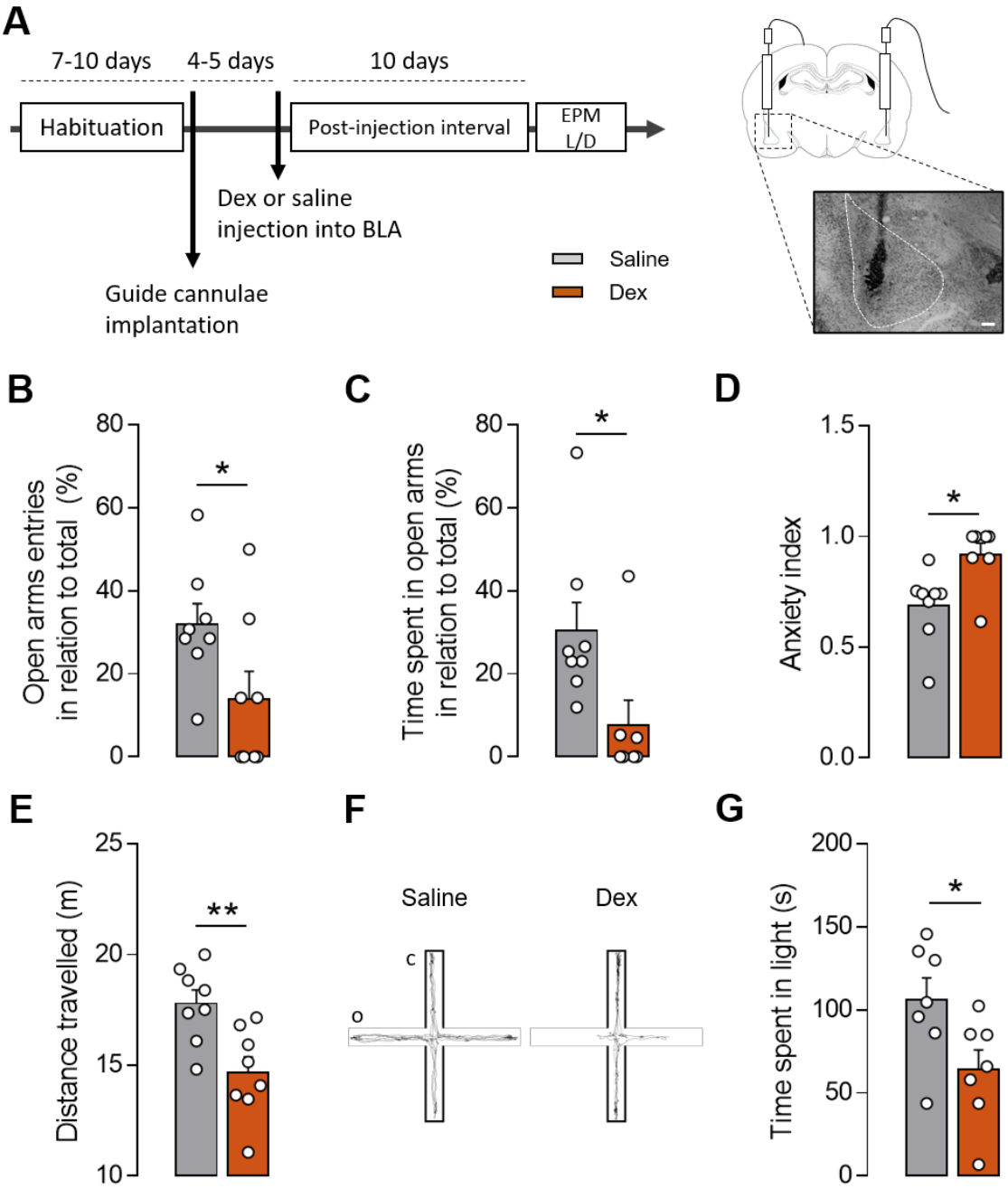

Figure 5. Intra-BLA dexamethasone administration promotes a anxiety-like behavior ten days after infusion. (A, left) Schematic representation of the experimental design showing the timeline of dexamethasone (Dex) or saline injection into BLA, the stress submission, and the behavioral tests. (Right) Representative figure and photomicrography showing a representative location of cannulae and injection needle tips into BLA. (Scale bar, 100 μm); (B–D) Intra-BLA dexamethasone administered animals exhibited reduced open arms entries (B; n = 8 animals per group, two-tailed student´s t-test: P = 0.0482) and time spent (C; n = 7-8 animals per group, two-tailed student´s t-test: P = 0.0285), as well as increased anxiety

index (D; n = 7-8 animals per group, two-tailed student´s t-test: P = 0.0127) in the EPM test comparing to saline administered animals. (E) Intra-BLA dexamethasone promoted a delayed reduced motor activity in the EPM test (n = 8 animals per group, two-tailed student's t-test: P = 0.0048). (F) Intra-BLA dexamethasone administration promoted a delayed decrease in time spent in the lit compartment comparing to saline administered animals in the light/dark (L/D) test (n = 7 animals per group, two-tailed student's t-test: P = 0.0369). (G) Representative tracking plots for the average motion of each experimental group in the EPM. Results are represented as mean ± SEM. Significance differences between groups are indicated as * P < 0.05.

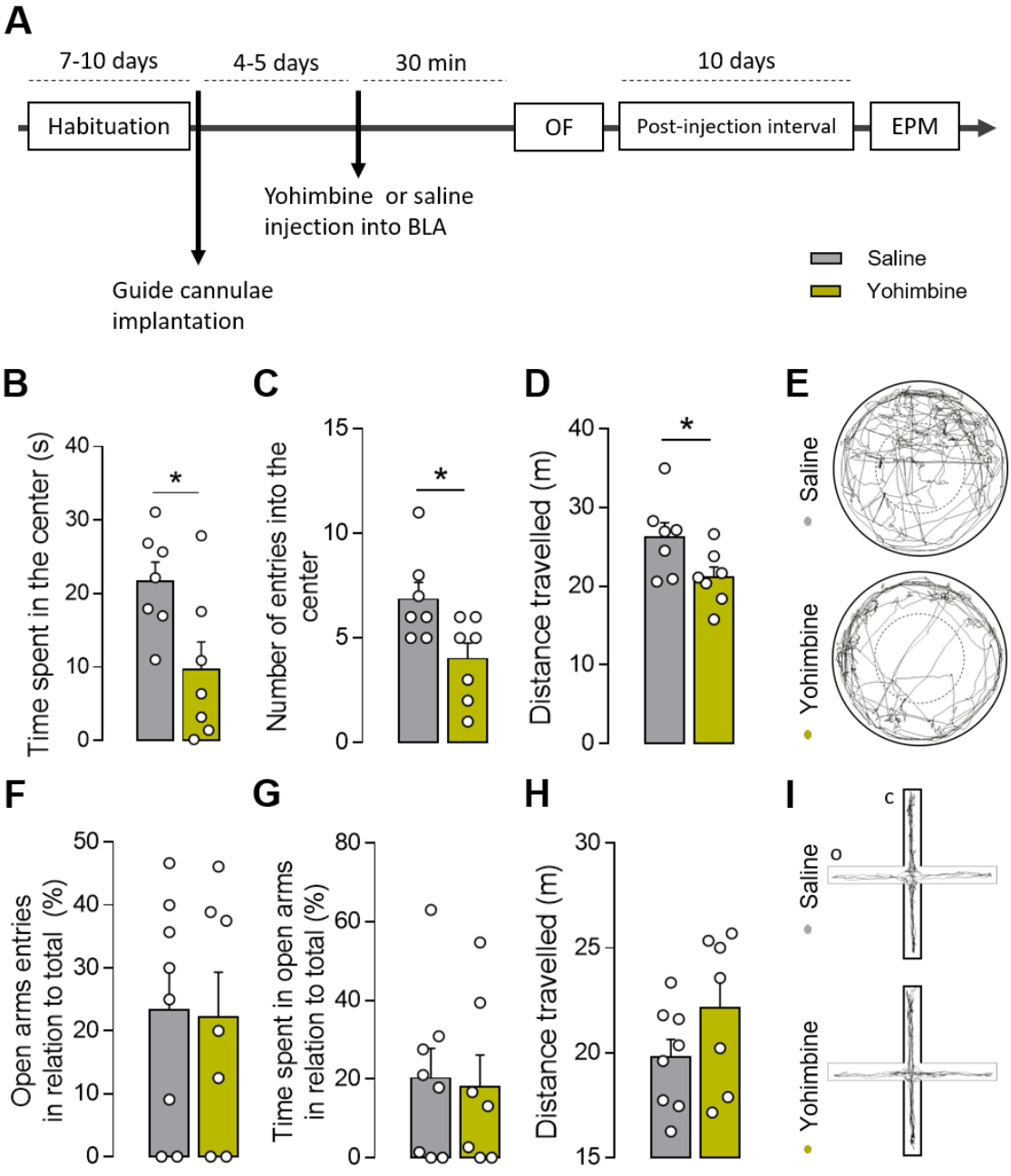

Figure 6. Intra-BLA yohimbine administration promotes an acute, but not delayed, anxiety-like behavior. (A, left) Schematic representation of the experimental design showing the timeline of yohimbine or saline injection into BLA and the behavioral tests. (Right) Representative figure and photomicrography showing a representative location of cannulae and injection needle tips in the BLA. (B-C) Animals that received intra-BLA yohimbine exhibited reduced time spent (B; n = 7 animals per group, two-tailed student´s t-test: P = 0.0225) and entries (C; n = 7 animals per group, two-tailed student´s t-test: P = 0.0234) in the center area of the OF. (D) Intra-BLA yohimbine promoted an acute decrease in motor activity in the OF (n = 7 animals per group, two-tailed student's t-test: P = 0.00462). (E)

894 Representative tracking plots for the average motion of each experimental group in the OF.
895 (F-G) There were no differences in the open arms entries (F; n = 7-8 animals per group, two-
896 tailed student´s t-test: P = 0.9058) and time spent (G; n = 7-8 animals per group, two-tailed
897 student´s t-test: P = 0.8491) in the EPM test of BLA yohimbine administered animals
898 comparing to saline administered animals. (H) Intra-BLA yohimbine did not influence the
899 animal's locomotor activity in the EPM (n = 7-8 animals per group, two-tailed student´s t-test:
900 P = 0.1617). (I) Representative tracking plots for the average motion of each experimental
901 group in the EPM. Results are represented as mean ± SEM. Significance differences between
902 groups are indicated as * P < 0.05.

903

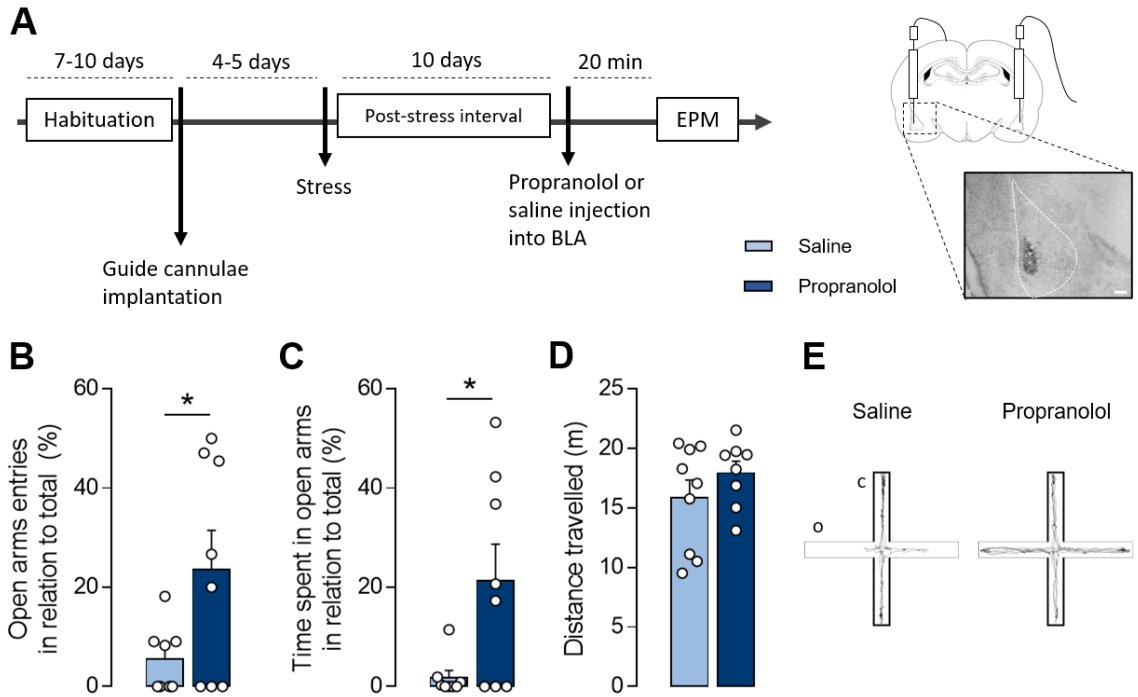

Figure 7. Pre-EPM test propranolol administration in the BLA prevented the delayed manifestation of the stress-induced anxiety-like behavior. (A, left) Schematic representation of the experimental design shows the propranolol or saline injection timeline into BLA, the stress submission, and the EPM test. (Right) Representative figure and photomicrograph showing the representative location of cannulae and injection needle tips into the BLA. (B-E) Stressed, intra-BLA saline-administered animals exhibited reduced open arms entries (B; n = 8 animals per group, two-tailed Student's t-test: P = 0.0441) and time spent (C; n = 8 animals per group, two-tailed Student's t-test: P = 0.0218) in the EPM test compared to stressed, intra-BLA propranolol-administered animals. (D) There was no influence of intra-BLA propranolol administration on the animal's locomotor activity in the EPM (n = 8-9 animals per group, two-tailed Student's t-test: P = 0.0285). (E) Representative tracking plots for the average motion of each experimental group in the EPM. Results are represented as the mean ± SEM. Significant differences between groups are indicated as * P < 0.05.